BJP British Journal of Pharmacology

DOI:10.1111/bph.12055
www.brjpharmacol.org

RESEARCH PAPER

Targeted delivery of doxorubicin through conjugation with EGF receptor–binding peptide overcomes drug resistance in human colon cancer cells

Shibin Ai[1], Tao Jia[1], Weilun Ai[1], Jianli Duan[1], Yongmei Liu[1], Jing Chen[1], Xin Liu[1], Fan Yang[2], Yuan Tian[2] and Zebo Huang[1,3]

[1]*Key Laboratory of Combinatorial Biosynthesis and Drug Discovery, Ministry of Education*, and *School of Pharmaceutical Sciences, Wuhan University, Wuhan, China,* [2]*Union Hospital, Tongji Medical College, Huazhong University of Science and Technology, Wuhan, China, and* [3]*Research Center of Food and Drug Evaluation, Wuhan University, Wuhan, China*

Correspondence
Zebo Huang and Shibin Ai, School of Pharmaceutical Sciences, Wuhan University, Wuhan 430071, China. E-mail: zbhuang@whu.edu.cn; aishibin@tom.com

Keywords
doxorubicin; doxorubicin–peptide conjugate; drug delivery; drug resistance; EGF receptor

Received
30 March 2012
Revised
10 October 2012
Accepted
1 November 2012

BACKGROUND AND PURPOSE

Induction of multidrug resistance by doxorubicin (DOX), together with non-specific toxicities, has restricted DOX-based chemotherapy. Recently, we demonstrated that DOX conjugated with an EGF receptor-binding peptide (DOX-EBP) had enhanced anticancer efficacy and reduced systemic toxicity when targeting EGF receptor-overexpressing tumours. Here we investigated whether DOX-EBP is able to overcome drug resistance and the underlying molecular mechanisms.

EXPERIMENTAL APPROACH

DOX-resistant SW480/DOX cells were derived from non-resistant SW480 cells by stepwise exposure to increasing concentrations of DOX, and P-glycoprotein overexpression induced by DOX was confirmed by Western blotting. Cytotoxicity and intracellular distribution of drugs were evaluated by MTT assay and fluorescence microscopy respectively. EGF receptor-mediated endocytosis was determined in EGF receptor and endocytosis inhibition assays. Drug accumulation in tumour cells and murine xenografts was determined by HPLC.

KEY RESULTS

The cytotoxicity and accumulation of DOX-EBP in SW480/DOX cells were almost the same as in SW480 cells, but those of free DOX were reduced. DOX-EBP accumulation was prevented by inhibitors of both EGF receptors and endocytosis, suggesting EGF receptors mediate endocytotic uptake. Tumour accumulation of DOX-EBP was significantly higher than free DOX in mice, and the levels of DOX-EBP were similar in DOX-resistant and non-resistant tumour tissues. Importantly, DOX-EBP, but not free DOX, was effective at inhibiting solid tumour growth and increased survival rate in both sensitive and resistant models.

CONCLUSION AND IMPLICATIONS

DOX-EBP can overcome DOX resistance of tumour cells and increase *in vivo* antitumour efficacy. Therefore, it has the potential to be a potent therapeutic agent for treating drug-resistant cancers.

Abbreviations

ABC, ATP-binding cassette; DOX, doxorubicin; EBP, EGF receptor-binding peptide; MDR, multidrug resistance; NBD, nucleotide-binding domains; P-gp, P-glycoprotein; PAO, phenylarsine oxide; TMD, transmembrane domains

Introduction

One of the major causes leading to chemotherapeutic failure in cancer treatment is multidrug resistance (MDR), which involves increased efflux, decreased uptake and enzymatic deactivation of chemotherapeutic drugs. There is increasing evidence that an elevated expression of active drug transporters in the plasma membranes of cancer cells is a major resistance mechanism (Eckford and Sharom, 2009). These transporters belong to the ubiquitous superfamily of ATP-binding cassette (ABC) proteins, which are able to transport anticancer drugs across cell membranes using the energy of ATP binding and hydrolysis (Gottesman *et al.*, 2002; Al-Shawi *et al.*, 2003). Approximately 50 ABC transporters have been documented in humans, and about 15 such proteins have been shown, in *in vitro* experiments, to export chemotherapeutic drugs (Schinkel and Jonker, 2003). Among these transporters, only three have so far been found to act as major contributors to MDR in cancer: ABCB1 – P-glycoprotein (P-gp or MDR1), the first ABC protein whose structural data were obtained; ABCC1 – MDR-associated protein 1 (MRP1); and ABCG2 – breast cancer resistance protein (BCRP), also known as mitoxantrone resistance protein (MXR). These three proteins have been shown to be overexpressed in MDR cell lines in culture and have also been detected in MDR tumours in patients and thus appear to function as clinically relevant drug-efflux pumps (Eckford and Sharom, 2009). The efflux of cancer chemotherapeutics by these ABC pumps results in decreased intracellular drug concentration and, subsequently, reduced cytotoxicity. Intriguingly, the expression of an ABC transporter may be induced by a specific drug, but upon expression, it may also actively transport other drugs out of cells, leading to MDR (Rottenberg *et al.*, 2007).

It is known that multidrug ABC transporters are able to pump out a wide range of cytotoxic agents that share common features such as planar, heterocyclic, lipophilic and low molecular mass (Higgins, 2007). These cytotoxic drugs can rapidly distribute to the outer and inner leaflets of the plasma membrane, transport across the membranes by a flip-flop mechanism and partition into the cytoplasm (Regev *et al.*, 2005). However, as substrates of multidrug ABC proteins, these drugs can be pumped to the outer leaflet by the ABC drug-efflux pumps directly from the inner leaflet of the plasma membrane and then diffuse into the extracellular medium (Gatlik-Landwojtowicz *et al.*, 2006; Siarheyeva *et al.*, 2006; Aller *et al.*, 2009). Based on these observations, a number of studies have conjugated low molecular mass drugs to macromolecular carriers to overcome ABC-transporter-associated MDR of tumour cells (Meyer-Losic *et al.*, 2006; Wu *et al.*, 2006). In particular, drugs conjugated to peptides have been shown to alter the cellular uptake pathway and circumvent ABC-transporter-mediated drug efflux and thus are able to accumulate at high concentrations in drug-resistant cells, leading to improved therapeutic index and fewer adverse effects (Bajo *et al.*, 2003; Aroui *et al.*, 2010). For example, doxorubicin (DOX) conjugated with elastin-like polypeptide (ELP), a thermally responsive carrier, is shown to thermally target solid tumours and overcome drug resistance in cancer cells (Bidwell *et al.*, 2007). Cytoplasmic delivery of DOX by conjugation with cell-penetrating peptides TAT (CGGGYGRKKRRQRRR) and penetratin (CRQIKIWFQNRRM KWKK) can bypass the P-gp efflux pump and has significantly superior efficacy against drug-resistant tumour cells (Liang and Yang, 2005; Aroui *et al.*, 2010). An approach of particular interest to circumvent MDR is the targeting of cellular receptors by peptide-conjugated chemotherapeutic agents. Due to the aberrant overexpression of some receptors on the surface of malignant cells, high-affinity receptor-binding peptides targeting specific receptors can be used to deliver chemotherapeutic compounds directly to neoplastic cells, allowing the drug–peptide conjugates to be actively taken up by receptor-mediated endocytotic pathways and bypass ABC-transporter-mediated MDR. For example, the transferrin receptors are overexpressed in a variety of malignant cells, and the conjugation of DOX with transferrin can significantly increase the cytotoxic effect of DOX against tumour cells and overcome MDR in leukaemia cell lines (Łubgan *et al.*, 2009).

EGF receptors are overexpressed in a number of malignancies and thus provide a basis for selective ligand-based targeting of tumour cells. Since EGF is an important EGF receptor ligand with high binding affinity and selectivity for the EGF receptor, we have recently synthesized a DOX–peptide conjugate using the EGF receptor-binding region (CMYIEALDKYAC; EBP) of EGF. DOX is covalently coupled to EBP via an ester bond at position 14 of DOX through a glutarate spacer, and the DOX-EBP conjugate is shown to target tumour cells that overexpress EGF receptors, leading to enhanced anticancer efficacy and reduced systemic toxicity (Ai *et al.*, 2011). Because the EGF receptor is able to enter cells through an endocytotic process upon binding to a high-affinity ligand (Grandal and Madshus, 2008), drug delivery into EGF receptor-overexpressing cells via the EGF-EGF receptor complex may help overcome efflux pump-related resistance. Therefore, we investigated whether the DOX-EBP conjugate was able to overcome DOX resistance through receptor-mediated endocytotic uptake. We found that DOX-EBP bypassed the ABC drug-efflux pumps by altering the cellular uptake process and showed increased antitumour activity in DOX-resistant as well as non-resistant tumours.

Methods

Chemicals

Doxorubicin hydrochloride (DOX HCl) salt, daunorubicin hydrochloride, glutaric anhydride and phenylarsine oxide (PAO) were purchased from Sigma-Aldrich (St. Louis, MO). The DOX-EBP conjugate was synthesized as previously described (Ai *et al.*, 2011).

Cell cultures and animals

The human colon cancer cell line SW480 was obtained from the China Centre for Type Culture Collection (Wuhan, China) and grown in RPMI 1640 medium (Gibco BRL, Grand Island, NY), containing 10% FBS (Hyclone, Logan, UT), 10^5 U·L^{-1} penicillin and 100 mg·L^{-1} streptomycin at 37°C in a humidified atmosphere of 5% CO_2 and 95% air. The DOX-resistant cells were derived from non-resistant SW480 cells by stepwise exposure to increased concentrations of DOX (0.01,

0.02, 0.04, 0.08, 0.16, 0.32 and 0.50 μg·mL^{-1} in normal medium) as described previously (Ogawara *et al.*, 2009). After repeated induction for 6 months, the cells with resistance to DOX (i.e. SW480/DOX cells) were obtained and maintained in the presence of 0.32 μg·mL^{-1} DOX. Athymic male nude mice (BALB/c-nu/nu; 5–6 weeks old, 18–20 g) were obtained from the Experimental Animal Centre of Tongji Medical College, Huazhong University of Science and Technology (Wuhan, China) and maintained under pathogen-free conditions with a 12 h light/12 h dark cycle. All studies involving animals are reported in accordance with the ARRIVE guidelines for reporting experiments involving animals (Kilkenny *et al.*, 2010; McGrath *et al.*, 2010).

MTT assay

To examine the levels of drug resistance, SW480 and SW480/DOX cells were seeded in 96-well plates at a density of 5000 cells per well, and the cytotoxicity of free DOX and DOX-EBP conjugate was evaluated using the MTT assay as described previously (Lee *et al.*, 2005). After treatment with different concentrations of DOX or DOX-EBP at 37°C for 5 h and 48 h, 20 μL of MTT solution (5 mg·mL^{-1}) was added to each well and further incubated for 4 h. The culture medium was then removed, and 100 μL of DMSO was added to each well. After 20 min of incubation, the absorbance was measured using a microplate reader (Bio-Rad Model 450, Hercules, CA) at 570 nm (test wavelength) and 630 nm (reference wavelength).

LDH release assay

DOX-induced cell death in SW480 and SW480/DOX cell cultures was also assessed using an LDH assay, as described previously (Riganti *et al.*, 2005), which quantifies LDH released from cells into culture medium. Briefly, the cells were seeded in 24-well plates and grown until about 80% confluence. After the medium was removed, the cells were incubated with increasing concentrations of DOX or DOX-EBP for the times indicated. Cell-free supernatants from the cultures were collected and transferred to 96-well plates for measurement of LDH activity using an LDH cytotoxicity detection kit (Roche Diagnostics GmbH, Mannheim, Germany) according to the manufacturer's instructions. Maximal LDH release was obtained by treating control cells with 1% Triton X-100 for 10 min at room temperature and was used for calculating the percentage of LDH release, i.e. activity of released LDH in a treated sample over the activity of maximal LDH released in the control.

Determination of DOX content

Intracellular accumulation of DOX and DOX-EBP in SW480 and SW480/DOX cells was analysed by HPLC using an ODS-C18 analytical column (5 μm particle size, 250 × 4.6 mm, Thermo Scientific, Waltham, MA, USA), and the cellular drug content was shown as pg DOX per cell (Ai *et al.*, 2011).

ATPase assay

ATPase activity of membrane vesicle suspensions from SW480 and SW480/DOX cells was determined by measuring the release of inorganic phosphate (Pi) from ATP as described previously (Litman *et al.*, 1997) with modifications, using purified membrane vesicles from virus-infected Sf9 cells (BD Biosciences, Bedford, MA) as a reference. Membrane vesicle samples (20 μg protein per well) were incubated with 50 μL of 10 mM $MgCl_2$, 40 mM 3-(N-morpholino) propane sulfonic acid (MOPS)-Tris (pH 7.0), 50 mM KCl, 5 mM dithiothreitol, 0.1 mM EGTA, 4 mM sodium azide, 1 mM ouabain, 5 mM ATP and increasing concentrations of DOX or DOX-EBP at 37°C for 40 min, with or without 0.5 mM vanadate, which inhibited 100% of P-gp ATPase activity. The absorbance of released Pi was read using a microplate reader (Bio-Rad Model450). Results are expressed as vanadate-sensitive ATPase activities of the membrane vesicles.

Western blot analysis

Western blotting was performed essentially as described previously (Wong *et al.*, 2006). Briefly, SW480 and SW480/DOX cells were grown to 80% confluence in 25 cm^2 culture flasks (~1 × 10^7 cells per flask), washed and centrifuged. The pellet was dispersed in a lysis buffer containing 50 mM Tris–HCl (pH 7.4), 120 mM NaCl, 1 mM EDTA, 1% TritonX-100 and 1% (v/v) protease inhibitor cocktail (Sigma-Aldrich). The cell lysate was collected after centrifugation, and the protein concentration was determined using the Bio-Rad Detergent Compatible Protein Assay kit (Bio-Rad). Equal amount of proteins (20 μg per lane) from each sample was used for SDS-PAGE and transferred to PVDF membranes (Millipore, Bedford, MA). The membranes were blocked overnight at 4°C with Tris-buffered saline containing 0.05% (v/v) Tween-20 (TBS-T) and 5% (m/v) nonfat dried milk, and incubated for 1 h at room temperature with primary antibodies specific for P-gp (C219 monoclonal antibody, Signet Laboratories, Dedham, MA), MRP1 (MRPm6 monoclonal antibody, Kamiya Biomedical Corp., Seattle, WA), MRP2 (M_2III-6 monoclonal antibody, Alexis Corp., San Diego, CA) and BCRP (BXP-21 monoclonal antibody, Alexis Corp.). The membranes were washed with TBS-T and incubated for 1 h at room temperature with HRP-conjugated secondary antibody (Amersham Life Sciences, Cleveland, OH). Protein bands were visualized using an enhanced chemoluminescence kit (Amersham Biosciences, Piscataway, NJ). Monoclonal antibody β-actin AC-40 (Sigma-Aldrich) was used as a reference.

Annexin V/PI assay

Apoptosis was analysed in SW480 and SW480/DOX cells treated with DOX or DOX-EBP by flow cytometry using Annexin V-fluoresce in isothiocynate (Annexin V-FITC) and propidium iodide (PI) double staining method as described previously (Yamochi *et al.*, 2005). The cells were grown in 25 cm^2 culture flasks with normal medium to ~80% confluence (1 × 10^7 cells per flask) and then incubated with 5 mL of serum-free medium containing 1 μM of DOX or DOX-EBP conjugate at 37°C for indicated times. After being stained with Annexin V-FITC and PI, the cells were analysed with a flow cytometer (FACS Calibur; Becton-Dickinson, Rutherford, NJ, USA).

TUNEL assay

Apoptotic nuclei were detected by TUNEL method, which examines DNA strand breaks during apoptosis, using an *in situ* cell death detection kit (Roche Diagnostics GmbH) as described previously (Zhang *et al.*, 2011). After 24 h of incu-

bation with 1 μM of DOX or DOX-EBP conjugate, SW480 or SW480/DOX cells were washed with PBS. Cells on slides were fixed with 4% paraformaldehyde in PBS for 1 h at room temperature, permeabilized with 0.1% Triton X-100 in 0.1% sodium citrate for 2 min on ice and then labelled by TUNEL reaction according to the manufacturer's instructions. Cell nuclei were identified by DAPI (Sigma-Aldrich) staining. The slides were examined under fluorescence microscopy (Fluoview FV300, Olympus, Japan).

EGF receptor inhibition assay

SW480 and SW480/DOX cells were grown in 25 cm^2 culture flasks with normal medium to ~80% confluence (1×10^7 cells per flask), and an EGF receptor inhibition assay was performed as described previously (Ai *et al.*, 2011). Briefly, after pretreatment with 5 $\mu g \cdot mL^{-1}$ of anti-EGF receptor monoclonal antibody C225 (ImClone Systems, Inc., New York, NY) for 12 h and removal of the pretreatment solution, the cells were incubated with 0.5 μM of free DOX or DOX-EBP for the times indicated and then the cellular DOX content was determined by HPLC. The reduced cellular accumulation induced by C225 was used as an inhibition index of cellular DOX uptake.

Endocytosis inhibition assay

The effect of PAO, an inhibitor of receptor-mediated endocytosis, on the cellular accumulation of DOX-EBP conjugate was assessed essentially as described previously (Bild *et al.*, 2002). SW480 and SW480/DOX cells were grown in 25 cm^2 culture flasks with normal medium to ~80% confluence (1×10^7 cells per flask) and then incubated with 5 mL of serum-free medium containing 5 μM PAO and 0.5 μM free DOX or DOX-EBP conjugate at 37°C for the times indicated. Cellular DOX content was measured by HPLC, and the accumulation of free DOX and DOX-EBP was compared in the presence and absence of PAO.

Fluorescence microscopy

SW480 and SW480/DOX cells were grown on glass coverslips in 24-well plates, treated with 0.5 μM free DOX or DOX-EBP conjugate (prepared in serum-free RPMI-1640 medium before use) at 37°C for the times indicated and examined under a laser scanning confocal fluorescence microscope (Fluoview FV300, Olympus) at λ_{ex} = 480 nm and λ_{em} = 580 nm. Nuclei were visualized at λ_{ex} = 350 nm and λ_{em} = 460 nm after staining with 1 $\mu g \cdot mL^{-1}$ of DAPI (Sigma-Aldrich) at room temperature for 10 min (Abbosh *et al.*, 2006). To characterize the cellular uptake of DOX-EBP conjugate mediated by the EGF receptor pathway, the cells were pre-incubated with C225 for 12 h at 37°C. Following removal of pretreatment solution, the cells were washed with serum-free medium, incubated with free DOX or DOX-EBP at 37°C for the times indicated and visualized using the confocal microscope.

Colocalization assays with endocytotic markers

SW480 and SW480/DOX cells were grown on glass coverslips in 24-well plates for 24 h. After incubation with DOX-EBP conjugate for the times indicated, the cells were washed with PBS, fixed with 4% paraformaldehyde in PBS (pH 7.4) for 20 min and then permeabilized with 0.1% Triton X-100 in PBS for 30 min at room temperature. After being blocked with 5% BSA for 30 min, the samples were incubated with antibodies against early endosomal antigen (EEA)-1 (BD Biosciences) and lysosomal-associated membrane protein (LAMP)-1 (BD Biosciences) according to the manufacturer's specifications. Aminomethylcoumarin (AMCA)- and FITC-labelled conjugated secondary antibodies were used for visualization by confocal microscopy.

Determination of maximum tolerated dose (MTD) in health mice

To define the appropriate doses of free DOX and DOX-EBP conjugate, tumour-free male mice (4 per group) were used to determine the MTD in three cycles of single administration by i.v. injection at 7 day intervals. Each mouse was weighed and the average weight of a group was used to calculate the dose. MTD was defined as the dose leading to a reversible loss of 10% initial weight within 35 days after the first i.v. injection.

Tumour xenograft in mice

In order to perform drug accumulation and antitumour assays *in vivo*, SW480/DOX cells growing exponentially were used to generate DOX-resistant tumour xenograft. Mice were inoculated s.c. with 1×10^7 cells in both flanks, and the size of the tumour was measured twice weekly using calipers. As a control, the xenograft of a non-resistant tumour was also established by injecting SW480 with 1×10^7 cells into flanks of mice. Four weeks after tumour inoculation, the mice with size-matched tumours were aseptically dissected. The resultant tumours were excised, minced mechanically to 3 mm^3 pieces and transplanted s.c. into experimental animals by a trocar needle. The animals were randomized to treatment groups when tumours reached an appropriate size.

In vivo *evaluation of drug accumulation in tumour*

The *in vivo* accumulation of DOX-EBP in DOX-resistant and non-resistant tumour xenografts in athymic nude mice was assessed and compared with that of free DOX. When tumours reached a mean volume of ~550 mm^3, the mice were randomly divided into groups, each contained 48 animals. Free DOX or DOX-EBP conjugate (5 $mg \cdot kg^{-1}$ DOX or equivalent) was injected i.v. at a single drug dose. At selected time points (0.5, 1, 2, 4, 8, 12, 24 and 48 h) after the injection, the mice were killed by cervical dislocation, and tumour masses were removed, weighed and washed with cold PBS. The tumour samples were homogenized in an Ultra-Turrax T18 Homogenizer (IKA, Staufen, Germany). The concentration of DOX or DOX-EBP was determined by HPLC and quantified by comparison with a standard DOX curve. Tumour tissues from saline-injected mice were used as controls.

Antitumour activity assay in vivo

Nude mice bearing SW480 and SW480/DOX xenografts (six per group) were injected once with free DOX (2 $mg \cdot kg^{-1}$; MTD of 80%), DOX-EBP conjugate (15 $mg \cdot kg^{-1}$ DOX equivalent) or saline into the tail vein at days 7, 14 and 21 after transplantation of tumours. Animal survival was monitored daily, and

tumour size was measured twice weekly by using a caliper to measure length (a) and width (b). Inhibitory effects/activity on the tumour were assessed by measuring tumour size, which was calculated as volume (mm^3) = $(a \times b^2)/2$. The mice were monitored for up to 60 days after transplantation of tumours or killed earlier if (1) the mouse was lethargic or sick and unable to feed, (2) the tumour was >2.0 cm in any dimension, (3) the body weight decreased below 15% of initial weight. On day 60, most surviving mice were killed; however, if any of the surviving mice had palpable tumours on day 60, they were monitored until day 90 and then killed. Survival data are presented in a Kaplan–Meier plot.

Statistical analysis

Data are presented as mean ± SD and evaluated by Student's *t*-test using SPSS 13.0 for Windows (SPSS Inc., Chicago, IL, USA). Probability values of $P < 0.05$ were considered to be significant.

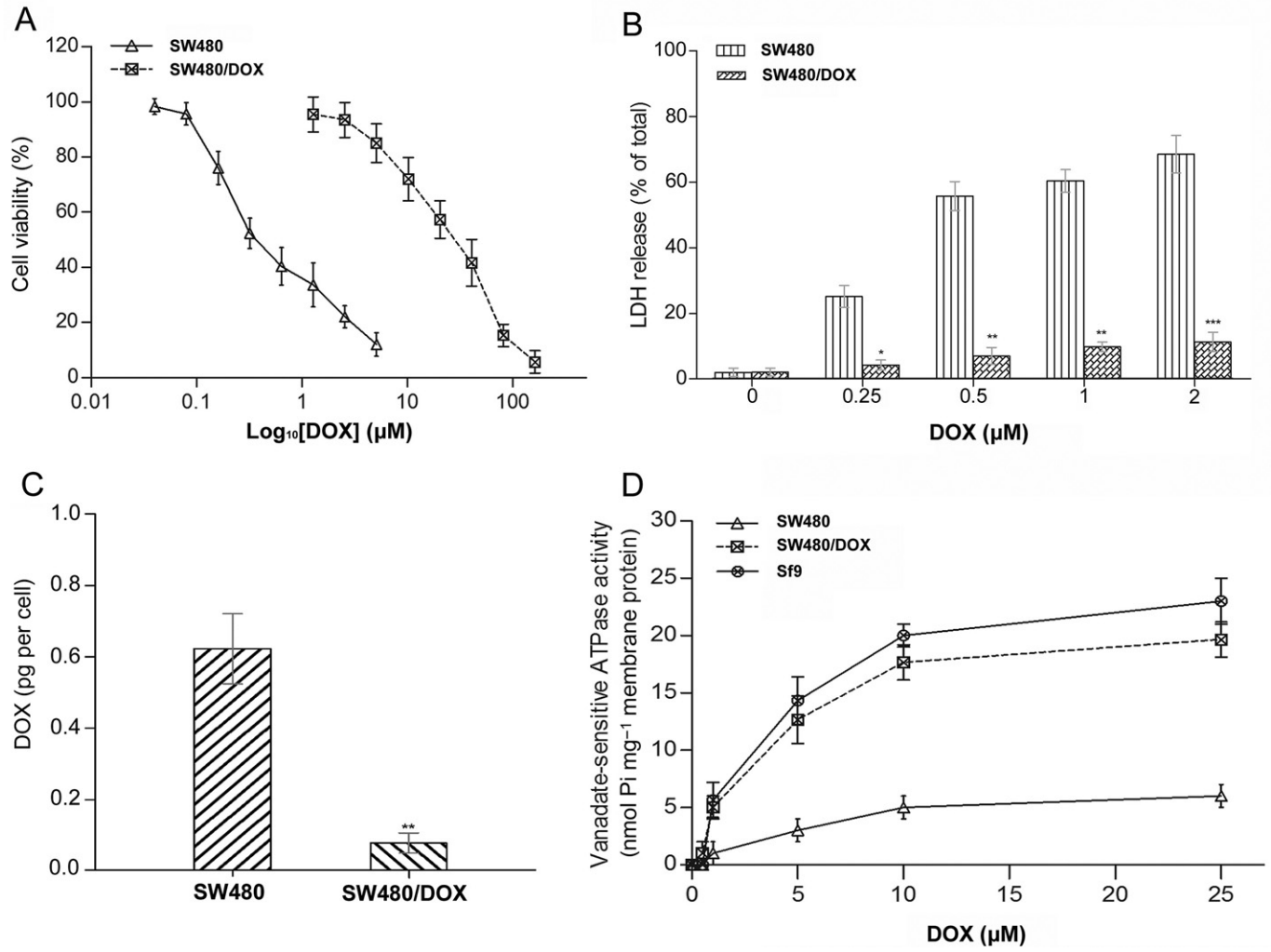

Figure 1

Cytotoxic effects and accumulation levels of free DOX in SW480 and SW480/DOX cells. (A) Cytotoxicity of free DOX on SW480 and SW480/DOX cells. The cells in 96-well plates were treated with a series of concentrations of free DOX at 37°C for 48 h, and cell viability was assessed by MTT method. Data are representative of three independent experiments and shown as mean ± SD ($n = 12$). (B) Effect of free DOX on the release of LDH from SW480 and SW480/DOX cells. Cells were incubated in 24-well plates with a series of concentrations of free DOX at 37°C for 48 h before determination of LDH release. Measurements were done in duplicate, and data are presented as mean ± SD ($n = 4$). *$P < 0.05$, **$P < 0.01$ and ***$P < 0.001$ (SW480/DOX vs. SW480 cells). (C) Cellular levels of free DOX accumulated in SW480 and SW480/DOX cells. The cells in 25 cm^2 culture flasks (~80% confluence) were treated with 0.5 μM free DOX in fresh serum-free medium at 37°C for 12 h, washed with ice-cold PBS three times and counted using a Coulter counter. After addition of daunorubicin as an internal standard, the cell pellet was extracted with an equal volume of chloroform and isopropanol mixture (3:1, v/v). DOX content was quantified by HPLC and expressed as pg per cell. **$P < 0.01$ (SW480 vs. SW480/DOX cells). (D) Effect of free DOX on the vanadate-sensitive ATPase activity in SW480 and SW480/DOX cells. Membrane preparations containing 20 μg of total proteins were incubated at 37°C for 40 min in the presence of free DOX at the indicated concentrations, and the release of inorganic phosphate (Pi) from ATP was measured. Purified membrane vesicles from virus-infected Sf9 cells were used as a reference.

Results

Resistance of SW480/DOX cells to free DOX

To address the problem of drug resistance in cancer chemotherapy, it is essential to compare the effects of a drug on both resistant and non-resistant cells. Therefore, we derived DOX-resistant SW480/DOX cells from its non-resistant parental SW480 cells by stepwise exposure to increased concentrations of DOX. To compare their sensitivity to DOX, both types of cells were exposed to a series of concentrations of free DOX, and cell viability was determined using the MTT method. After incubation with free DOX for 48 h, 2.5 μM DOX was very effective at inhibiting the proliferation of SW480 cells (~80% inhibition), but the same concentration had almost no cytotoxic effects on SW480/DOX cells (only ~7% inhibition) (Figure 1A), indicating a strong resistance of SW480/DOX cells to free DOX. To further confirm this resistance, we evaluated the cytocidal effect of free DOX on both SW480 and SW480/DOX cells using the LDH release assay (monitoring extracellular LDH activity), which is a sensitive indicator of cell death and a widely used marker in cytotoxicity studies. As shown in Figure 1B, free DOX was potent at killing SW480 cells but much less effective on SW480/DOX cells, causing about 60 and 10% LDH release, respectively, after a 48 h treatment with 0.5–2 μM DOX. This further demonstrates the DOX resistance of SW480/DOX cells.

To examine the cause of the acquired resistance, both SW480 and SW480/DOX cells were treated with 0.5 μM free DOX, and the cellular accumulation of DOX was determined by HPLC. As shown in Figure 1C, the DOX level in SW480/DOX cells was >8 times lower than that in SW480 cells after treatment with free DOX for 12 h, suggesting the DOX resistance of SW480/DOX cells was related to the lowered intracellular accumulation of free DOX. Since one of the most likely scenarios for intracellular DOX reduction in drug-resistant cells is the overexpression of ABC transport proteins, which can pump DOX out of the cells by use of the chemical energy of ATP hydrolysis, we measured the amount of Pi liberated from ATP, as the released Pi is directly proportional to and can be used as an indicator of ATPase activity. As shown in Figure 1D, DOX, a typical substrate of ABC transporters, produced a concentration-dependent increase in ATPase activity in membrane vesicles isolated from SW480/DOX cells, and the concentration required for 50% stimulation of ATPase activity was ~2.7 mM. Overall this was similar to the mode of action of DOX in the purified membrane vesicles from Sf9 insect cells, which are known to overexpress ABC proteins and widely used to detect the interaction of compounds with ABC transporters (Bakos *et al.*, 2000). In contrast, only a weak modulation of ATPase activity was found in the isolated membrane vesicles form SW480 cells. Together, these results strongly suggest that the lowered intracellular accumulation of free DOX in SW480/DOX cells was due to the overexpression of ABC transporter proteins.

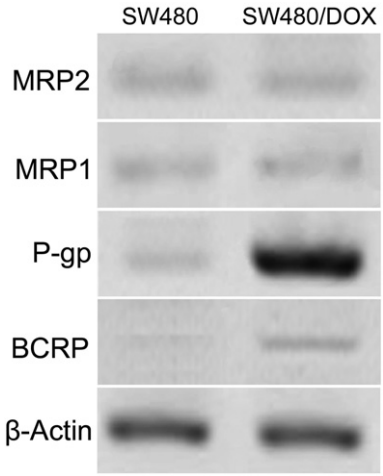

Figure 2

Western blot analysis of ABC transporter proteins in SW480 and SW480/DOX cells. Cell lysates were prepared from confluent cells grown at 37°C in 25 cm^2 culture flasks (~1×10^7 cells per flask). Equal amount of proteins (20 μg per lane) was separated by SDS-PAGE and analysed by Western blotting using monoclonal antibody C219 for P-gp, MRPm6 for MRP1, M_2III-6 for MRP2, BXP-21 for BCRP and AC-40 for β-actin.

Overexpression of P-gp in DOX-resistant SW480/DOX cells

In order to identify the ABC transporters involved in the resistance of SW480/DOX cells to free DOX, a number of ABC proteins, including MRP1, MRP2, P-gp and BCRP, was analysed by Western blotting. As shown in Figure 2, an overexpression of P-gp, but not of the other proteins tested, was

Table 1

IC_{50} values of free DOX and the DOX-EBP conjugate in SW480 and SW480/DOX cells

	IC_{50} of DOX equivalent (μM)			
	5 h		48 h	
Cells	Free DOX	DOX-EBP	Free DOX	DOX-EBP
SW480	12.45 ± 1.62	64.37 ± 2.68	0.56 ± 0.16	0.08 ± 0.03
SW480/DOX	329.28 ± 7.36	68.75 ± 2.25	32.85 ± 1.62	0.10 ± 0.06

Cells in 96-well plates (5×10^3 cells per well) were grown for 24 h and then incubated with increasing concentrations of free DOX or DOX-EBP for the indicated times. Cell viability was assessed by the MTT assay, and IC_{50} values were obtained by sigmoidal curve fitting of the data.

detected in the DOX-resistant SW480/DOX cells, while none of the proteins analysed was detected in the non-resistant SW480 cells, implying that P-gp contributes to the efflux of free DOX and thus to the DOX resistance of SW480/DOX cells.

Cytocidal efficacy of DOX-EBP conjugate against DOX-resistant SW480/DOX cells

Since both SW480 and SW480/DOX cells are capable of over-expressing EGF receptors (data not shown), they were used to evaluate the cytocidal potency of DOX-EBP on DOX-sensitive and -resistant cells. The cells were treated with the conjugate in a series of concentrations, and their cell viability was determined using the MTT assay. Although the cytotoxic effect of free DOX on the resistant SW480/DOX cells was very poor after a 48 h treatment (Figure 1A), the cytotoxicity of DOX-EBP conjugate on the same cell line was significantly increased (Figure 3A). Also, there was no significant difference in the inhibitory effects on cell proliferation induced by the conjugate between the resistant and non-resistant cell lines. To compare the results more directly, the IC_{50} values in both cell lines exposed to free DOX or DOX-EBP for 5 h and

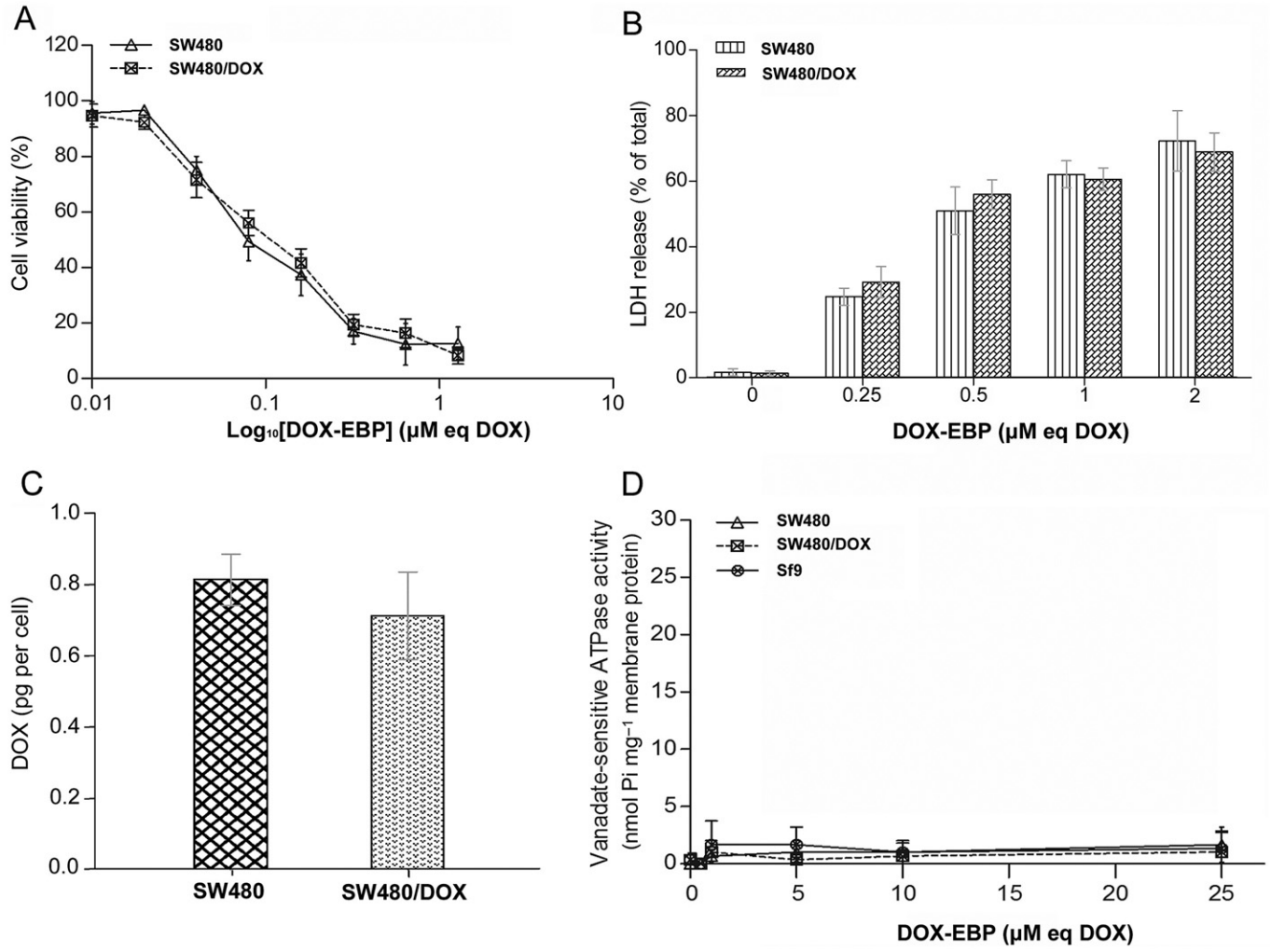

Figure 3

Cytocidal effects and accumulation levels of DOX-EBP conjugate in SW480 and SW480/DOX cells. (A) Cytotoxicity of DOX-EBP on SW480 and SW480/DOX cells. The cells in 96-well plates were treated with a series of concentrations of DOX-EBP at 37°C for 48 h, and cell viability was assessed by MTT method. Data are representative of three independent experiments and shown as mean ± SD (n = 12). (B) Effect of DOX-EBP on the release of LDH from SW480 and SW480/DOX cells. Cells were incubated in 24-well plates with a series of concentrations of DOX-EBP at 37°C for 48 h before determination of LDH release. Measurements were done in duplicate, and data are presented as mean ± SD (n = 4). (C) Cellular levels of DOX-EBP accumulated in SW480 and SW480/DOX cells. The cells in 25 cm^2 culture flasks (~80% confluence) were treated with 0.5 μM DOX-EBP in fresh serum-free medium at 37°C for 12 h, washed with ice-cold PBS three times and counted using a Coulter counter. After addition of daunorubicin as an internal standard, the cell pellet was extracted with an equal volume of chloroform and isopropanol mixture (3:1, v/v). Drug content was quantified by HPLC and expressed as pg per cell. (D) Effect of DOX-EBP on the vanadate-sensitive ATPase activity in SW480 and SW480/DOX cells. Membrane preparations containing 20 μg of total proteins were incubated at 37°C for 40 min in the presence of DOX-EBP at the indicated concentrations, and the release of inorganic phosphate (Pi) from ATP was measured. Purified membrane vesicles from virus-infected Sf9 cells were used as a reference.

48 h are summarized in Table 1, which shows that the IC_{50} values of the conjugate were very close in both types of cell, demonstrating a similar cytotoxic effect of DOX-EBP on both DOX-resistant and non-resistant cells. Importantly, the IC_{50} values of DOX-EBP were significantly lower than that of free DOX in the DOX-resistant SW480/DOX cells, at a comparable scale with that of free DOX in non-resistant SW480 cells, indicating the ability of DOX-EBP to counteract DOX resistance. In addition, using the LDH release assay we also demonstrated a significant increase in LDH release in SW480/DOX cells when treated with DOX-EBP as compared with free DOX (Figure 3B vs. Figure 1B) and confirmed that similar levels of LDH were released by DOX-EBP in SW480/DOX and SW480 cells (Figure 3B). This further supports the prevention of DOX resistance by the conjugate.

To investigate the cytocidal action of the conjugate, cellular DOX levels in SW480 and SW480/DOX cells were determined by HPLC, and comparable DOX accumulation levels were found in the two types of cells after treatment with 0.5 μM DOX-EBP for 12 h (Figure 3C). These results demonstrate that the DOX-EBP conjugate is capable of preventing drug resistance of SW480/DOX cells by increasing its accumulation level, as compared with that of free DOX (Figure 1C). Since DOX is a typical substrate of ABC transporter proteins, we tested whether the DOX-EBP conjugate is also such a substrate by measuring the ATPase activities of the isolated membrane vesicles from the SW480 and SW480/DOX cells after DOX-EBP treatment. In contrast to the patterns observed for free DOX (Figure 1D), no vanadate-sensitive ATPase activity was detected in either the membrane preparations of DOX-EBP-treated SW480 and SW480/DOX cells or the control Sf9 membrane vesicles (Figure 3D), suggesting that the conjugate does not have an significant interaction with ABC transporters.

It is known that apoptosis plays an important role in the cytotoxicity of DOX; thus, we examined whether apoptotic or necrotic cell death was induced by DOX-EBP. After 24 h of treatment with 1 μM DOX-EBP, about 30–50% of SW480 and SW480/DOX cells stained positive with Annexin V in FACS studies (Figure 4A), suggesting the cells were sensitive to the conjugate-mediated apoptosis. Further experiments with TUNEL staining revealed much more green fluorescence in SW480/DOX cells and also slightly more fluorescence in SW480 cells treated with DOX-EBP, as compared with those treated with free DOX (Figure 4B). These findings suggest that the death of SW480 and SW480/DOX cells induced by DOX-EBP at the concentrations tested (<5 μM) is attributable to apoptotic, rather than necrotic, cell death.

Intracellular distribution of DOX-EBP conjugate in DOX-resistant SW480/DOX cells

To examine the intracellular distribution of the DOX-EBP conjugate, both SW480 and SW480/DOX cells were incu-

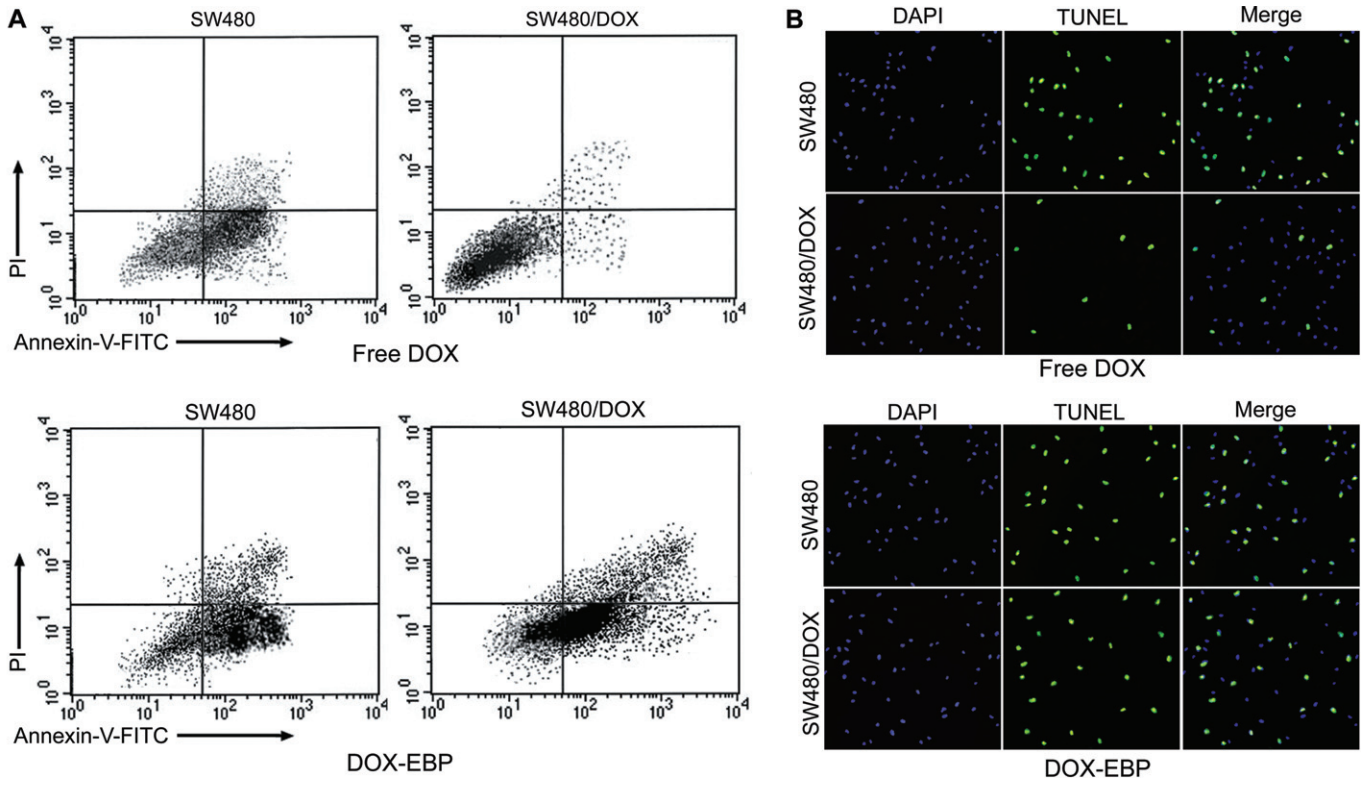

Figure 4

Effects of free DOX and DOX-EBP on apoptosis in SW480 and SW480/DOX cells. After incubation with 1 μM of free DOX and equivalent molar concentrations of DOX-EBP for 24 h, the cells were stained with Annexin V-FITC and PI to access the apoptotic potential by flow cytometry (A) and labelled with TUNEL/DAPI reaction to identify apoptotic cells under a confocal microscope (B).

bated with free DOX or the conjugate and their distribution evaluated by confocal fluorescence microscopy. The outlines of nuclei were identified by DAPI staining while the distribution of DOX and DOX-EBP was shown by DOX autofluorescence (Figure 5). After incubation with free DOX at 37°C for 30 min, the DOX fluorescence was clearly detected in both cytoplasm and nuclei of non-resistant SW480 cells, but only a weak fluorescent signal was observed in DOX-resistant SW480/DOX cells (Figure 5A). However, after incubation with DOX-EBP conjugate for the same period, the DOX fluorescence in cytoplasmic and perinuclear regions, although not in the nuclei, was comparable in both SW480 and SW480/DOX cells (Figure 5B).

After 24 h of incubation with free DOX, the intracellular distribution of the DOX signal in SW480 cells was almost the same as that after a 30 min incubation, and the fluorescent signal was still weak, although slightly increased, in SW480/DOX cells (Figure 5C). However, after the same period of incubation with the DOX-EBP conjugate, a much stronger DOX fluorescence in cytoplasm and nuclei was detected in both SW480 and SW480/DOX cells (Figure 5D), as compared with that of the 30 min treatment (Figure 5B), suggesting the DOX enters the nuclei after a prolonged incubation with the conjugate.

Cellular accumulation of DOX-EBP conjugate via EGF receptor-mediated endocytosis in DOX-resistantSW480/DOX cells

Previous studies have demonstrated that free DOX can diffuse easily across the cell membrane but may also be rapidly pumped out from DOX-resistant cells, while the conjugation of DOX to carrier molecules may circumvent this efflux effect of resistant cells (Bidwell *et al.*, 2007). Therefore, carrier-based DOX delivery systems, which may enter cellular compartments through receptor-mediated endocytosis, have been regarded as a primary method to bypass the efflux action of P-gp pumps (Kim *et al.*, 2008; Łubgan *et al.*, 2009). To test whether the DOX-EBP conjugate was transported via EGF receptor-mediated endocytosis, we performed assays in SW480 and SW480/DOX cells in which both EGF receptors and endocytosis were inhibited. The anti-EGF receptor monoclonal antibody C225 can competitively inhibit the binding

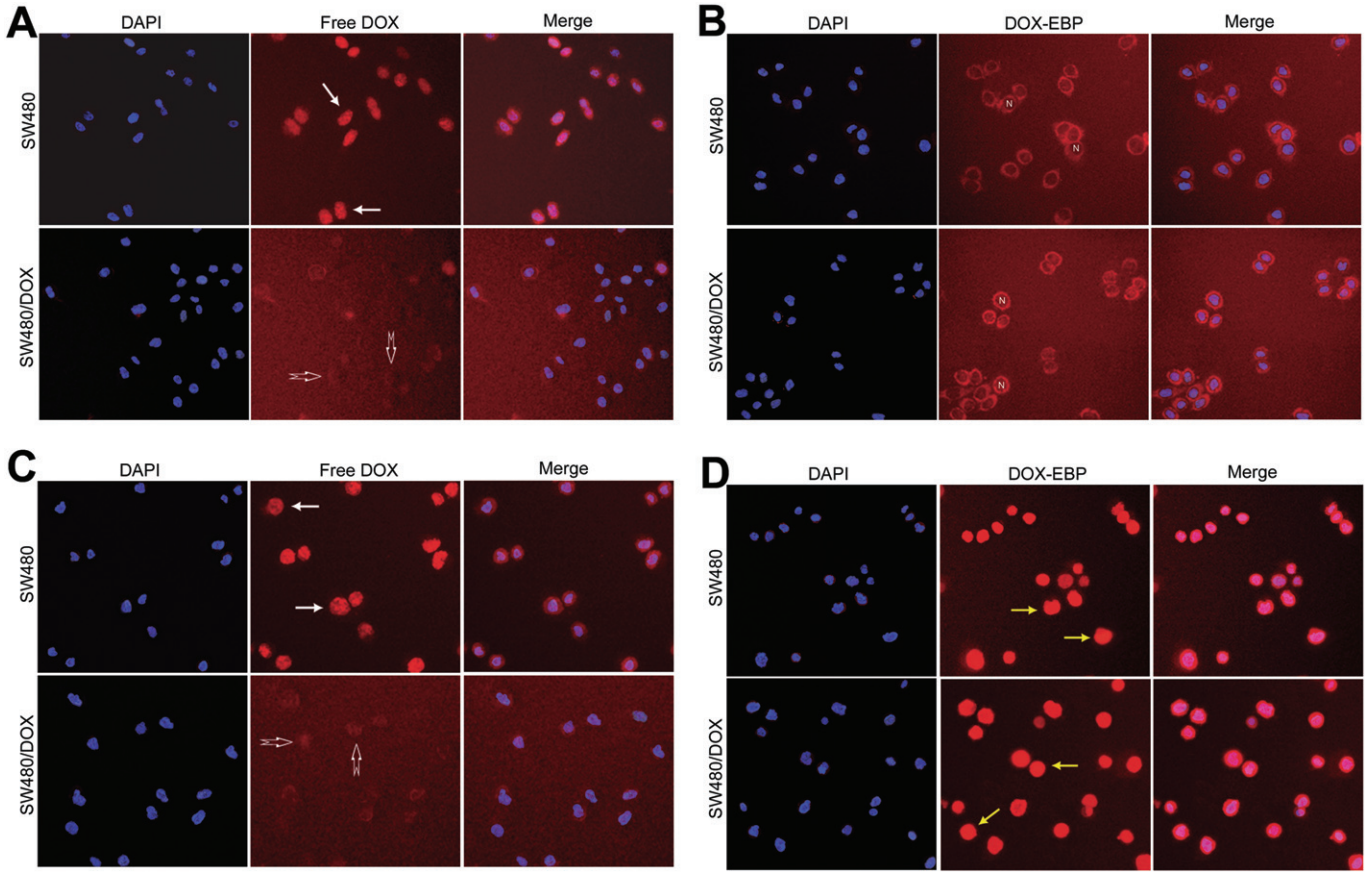

Figure 5

Intracellular distribution of free DOX and DOX-EBP conjugate in SW480 and SW480/DOX cells. The cells were incubated with 0.5 μM of free DOX or DOX-EBP in fresh serum-free medium at 37°C for 30 min (A and B) or 24 h (C and D) and visualized under a confocal fluorescence microscope. Merged images display the overlay of blue DAPI staining of nuclei and red autofluorescence of DOX, where purple represents DOX in the nuclear region. White solid arrow indicates cytoplasmic and nuclear fluorescence of drugs. Swallowtail arrow indicates cellular outline or indistinct intracellular fluorescence. N = nucleus. Yellow solid arrow indicates strong intracellular fluorescence, including both cytoplasm and nucleus.

of ligands to EGF receptors and block ligand-induced activation of the receptor (Lurje and Lenz, 2007) and thus was used to evaluate whether the DOX-EBP conjugate was mediated by EGF receptors. SW480 and SW480/DOX cells were pre-incubated with C225 before treatment with DOX-EBP or free DOX. As shown in Figure 6A, no significant difference in cellular DOX levels was found after 1 h of free DOX treatment with or without C225 pre-incubation in both SW480 and SW480/DOX cells. However, when the cells were treated with DOX-EBP conjugate for 1 h, the intracellular DOX accumulation was significantly reduced in both types of cell pre-incubated with C225 as compared with corresponding cells without C225 pre-incubation (Figure 6A). Similarly, after 12 h of treatment with free DOX or DOX-EBP, the cellular accumulation of free DOX was not changed by C225 pre-incubation, but that of DOX-EBP was significantly inhibited (~50%) in both SW480 and SW480/DOX cells (Figure 6B). These data suggest that the EGF receptor is involved in the delivery of DOX-EBP conjugate into the tumour cells.

PAO is a pharmacological inhibitor of endocytosis (Bild *et al.*, 2002) and thus was used to investigate whether the cellular entry of DOX-EBP conjugate was mediated by

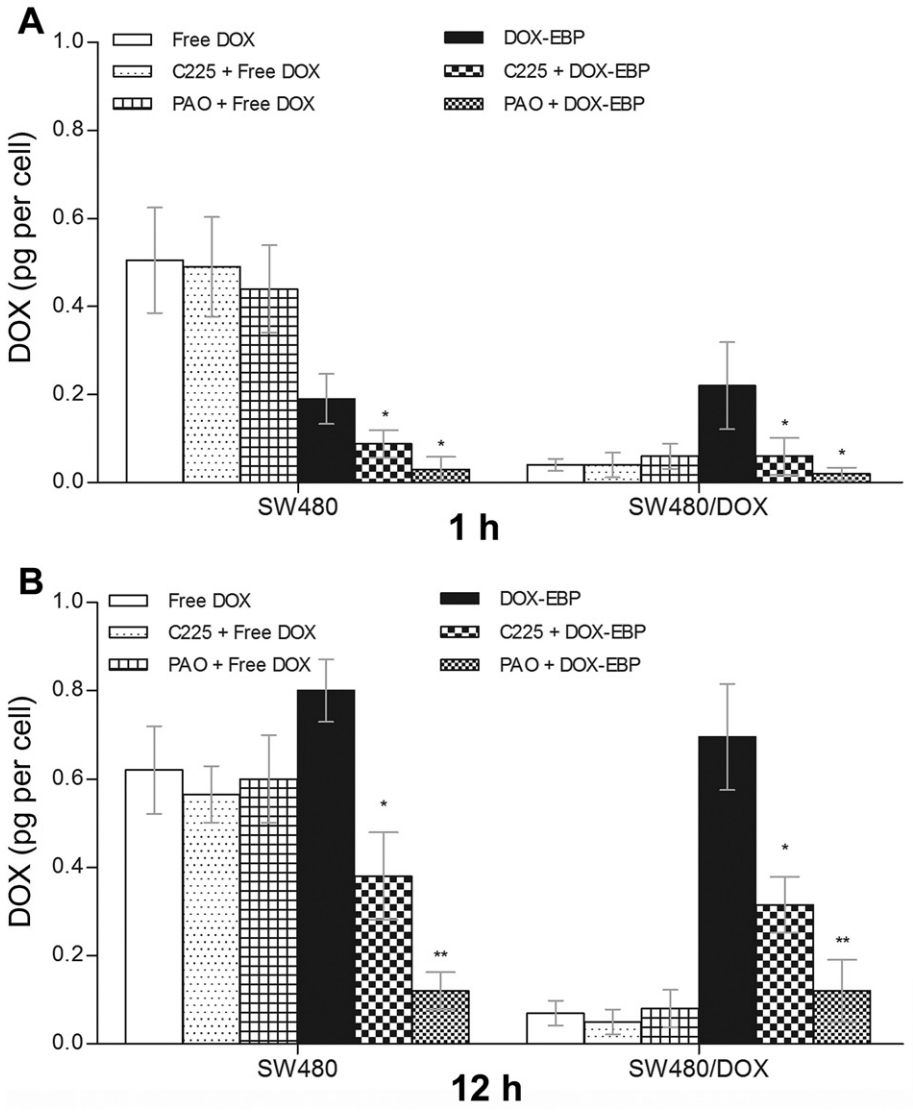

Figure 6

Effects of anti-EGF receptor antibody and endocytosis inhibitor on the accumulation levels of free DOX and DOX-EBP conjugate in SW480 and SW480/DOX cells. For EGF receptor inhibition assay, the cells in 25 cm^2 culture flasks (~80% confluence) were pretreated with 5 $\mu g \cdot mL^{-1}$ of anti-EGF receptor monoclonal antibody C225 in fresh serum-free medium at 37°C for 12 h and then incubated with 0.5 μM of free DOX or DOX-EBP in fresh serum-free medium for 1 h (A) or 12 h (B). In the endocytosis inhibition assay, the cells in 25 cm^2 culture flasks (~80% confluence) were treated with 0.5 μM of free DOX or DOX-EBP in the presence of 5 μM of the endocytosis inhibitor PAO at 37°C for 1 h (A) or 12 h (B). After addition of daunorubicin as an internal standard, the cell pellet was extracted with an equal volume of chloroform and isopropanol mixture (3:1, v/v). Drug content was quantified by HPLC and expressed as pg per cell. Data are shown as mean ± SD (n = 6). *P < 0.05, **P < 0.01.

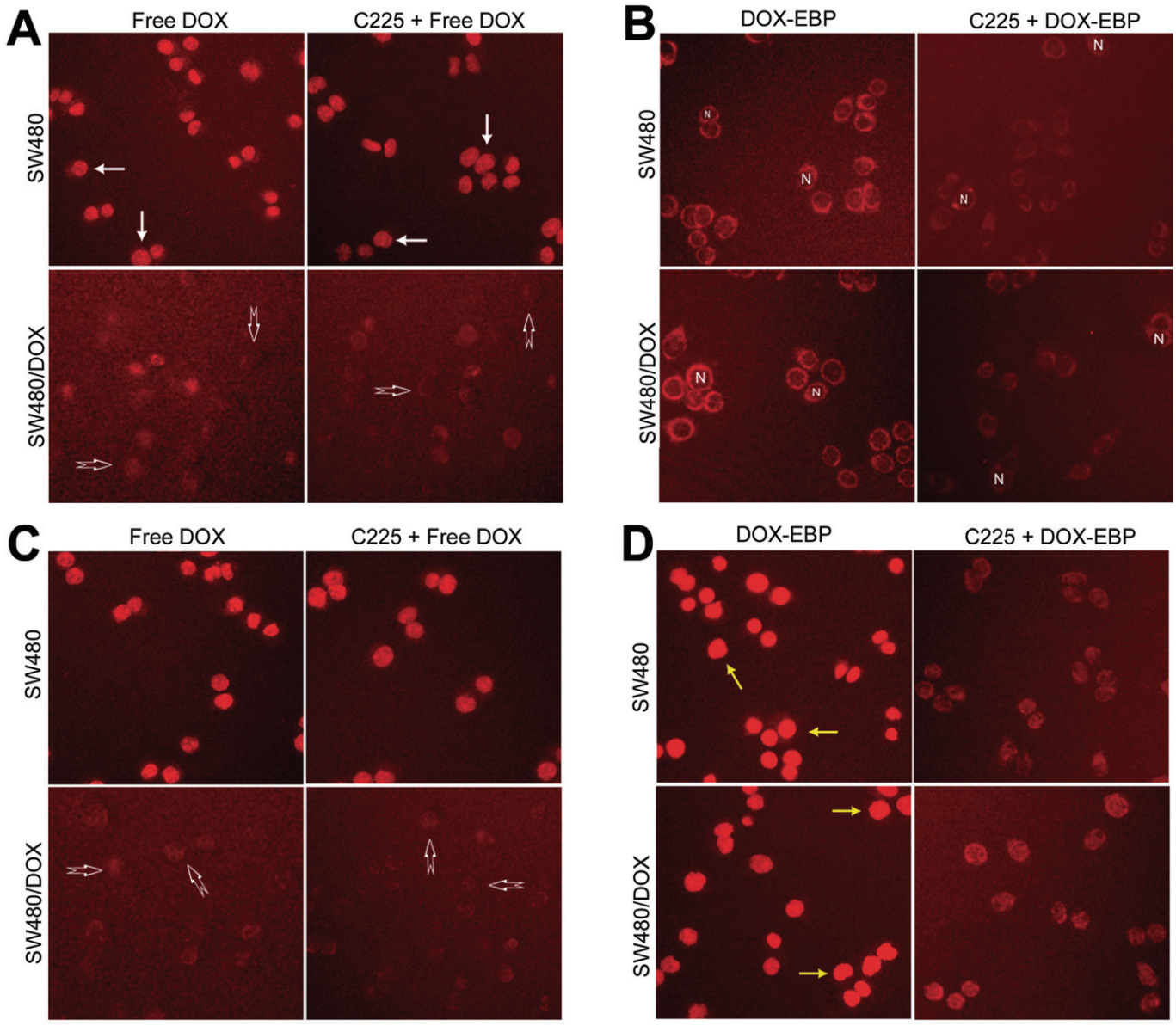

Figure 7

Effects of anti-EGF receptor antibody on the intracellular distribution of free DOX and DOX-EBP conjugate in SW480 and SW480/DOX cells. The cells were pretreated with or without 5 μg·mL^{-1} of anti-EGF receptor monoclonal antibody C225 in fresh serum-free medium at 37°C for 12 h and then incubated with 0.5 μM of free DOX or DOX-EBP in fresh serum-free medium for 30 min (A and B) or 24 h (C and D) before visualization under a confocal fluorescence microscope. White solid arrow indicates cytoplasmic and nuclear fluorescence of drugs. Swallowtail arrow indicates cellular outline or indistinct intracellular fluorescence. N = nucleus. Yellow solid arrow indicates strong intracellular fluorescence, including both cytoplasm and nucleus.

endocytosis. After 1 h of incubation with free DOX or DOX-EBP in the presence of PAO, the cellular accumulation of free DOX was not affected by PAO in either SW480 or SW480/DOX cells, but that of DOX-EBP was significantly reduced in both types of cell compared with non-PAO treatments (Figure 6A). Similar results were also found in both cell lines after 12 h of incubation with the drugs (Figure 6B). Taken together, these data suggest that the DOX-EBP conjugate is transported into and accumulates in the tumour cells via EGF receptor-mediated endocytosis, bypassing P-gp-mediated efflux.

EGF receptor-mediated endocytotic internalization of DOX-EBP conjugate in DOX-resistant SW480/DOX cells

To further investigate the cellular uptake process of DOX-EBP conjugate in DOX-resistant cells, both SW480 and SW480/

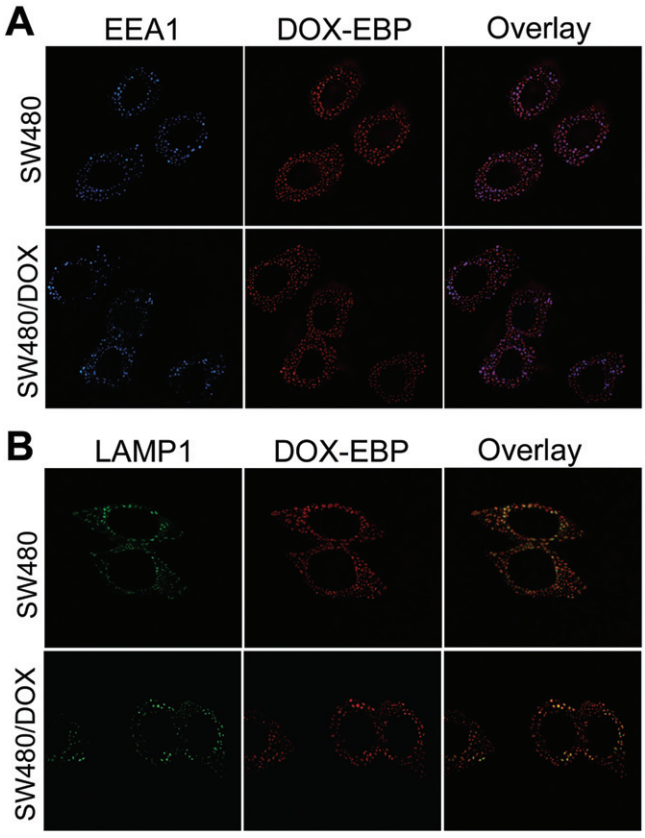

Figure 8

Colocalization of internalized DOX-EBP conjugate with endosomes and lysosomes. The SW480 and SW480/DOX cells were incubated with DOX-EBP, washed with PBS, fixed with paraformaldehyde and blocked with BSA. The early and late distribution of internalized DOX-EBP in endosomes (A) and endosomes/lysosomes (B) were stained, respectively, with anti-EEA1 and anti-LAMP1 antibodies and examined by confocal microscopy.

DOX cells were pretreated with C225 before incubation with free DOX or the conjugate and observed under confocal fluorescence microscope. As shown in Figure 7A, pretreatment with C225 had no effect on the intracellular fluorescent intensity and distribution of free DOX in either SW480 or SW480/DOX cells, indicating that free DOX entered cytoplasm and nucleus in a manner independent of EGF receptors after 30 min of incubation. When the cells were incubated with DOX-EBP conjugate for the same period, however, the intracellular fluorescence intensity in both types of cells was reduced by C225 pretreatment (Figure 7B), demonstrating the involvement of EGF receptors in cellular internalization of the conjugate. Similarly, pretreatment with C225 had no effect on the fluorescence distribution of free DOX (Figure 7C) but reduced the cellular fluorescence intensity of DOX-EBP (Figure 7D) when the cells were incubated with the drugs for 24 h. These data suggest that DOX-EBP conjugate entered the cells in an EGF receptor-dependent fashion, and that the conjugate was retained in both DOX-resistant and non-resistant cells.

Since the consequence of receptor-mediated internalization of a conjugated drug is its enclosure first in endosomes and then in lysosomes, where the conjugate is cleaved and released into the intracellular space, we performed colocalization experiments of internalized DOX-EBP using endosome and lysosome markers (labelled monoclonal antibodies against EEA1 and LAMP1, respectively) to assess whether endocytotic pathways are involved in the uptake of DOX-EBP conjugate. As shown in Figure 8, DOX-EBP was indeed colocalized with anti-EEA1-labelled intracellular structures 4 h after its uptake and then accumulated in LAMP1-positive lysosomes after 24 h in both in SW480 and SW480/DOX cells. These results suggest that endocytosis was involved in the post-internalization steps of DOX-EBP trafficking.

Increased accumulation of DOX-EBP conjugate in DOX-resistant tumours in vivo

The tumour accumulation of free DOX and DOX-EBP conjugate after i.v. administration at a single dose of 5 $mg \cdot kg^{-1}$ DOX equivalent for the indicated times was evaluated in both DOX-resistant and non-resistant tumour-bearing mice. As shown in Figure 9A, the peak level of free DOX in SW480 tumour tissue was 8 $\mu g \cdot g^{-1}$ at 0.5 h after injection, whereas that of DOX-EBP was 21 $\mu g \cdot g^{-1}$ at 8 h, a 2.5-fold increase in drug accumulation. The AUC (area under tumour tissue concentration–time curve) value of DOX-EBP in the tumour was also increased >6-fold more than that of free DOX, from 134 increased to 761 $\mu g \cdot h \cdot g^{-1}$, further suggesting a significantly higher tumour accumulation of DOX-EBP conjugate in the non-resistant tumour-bearing mice as compared with free DOX. On the other hand, the peak level and AUC were four and five times lower, respectively, in DOX-resistant tumour tissue than those in non-resistant tumour tissue after administration of free DOX (Figure 9A and B), indicating the resistance of the SW480/DOX tumour to free DOX *in vivo*. In contrast, the peak level of DOX-EBP in the DOX-resistant tumour tissue was almost the same as that in non-resistant tumour tissue (Figure 9A and B), and importantly the AUC from the administration of DOX-EBP was ~24-fold higher than that from free DOX in the DOX-resistant tumour tissue (Figure 9B). Together, these results suggest that the DOX-EBP conjugate may be therapeutically effective on both types of tumour.

Increased antitumour activity of DOX-EBP conjugate to DOX-resistant tumours in vivo

To determine the optimal dosing schedule for antitumour therapy, an *in vivo* MTD assay was performed in non-tumour bearing mice, and it was found that the MTD for free DOX and DOX-EBP were 2.5 and 80 $mg \cdot kg^{-1}$ respectively. A dose–response experiment was also conducted by monitoring tumour growth, survival rate and body weight change of BALB/c-nu/nu mice treated with well-tolerated doses of free DOX and DOX-EBP on days 7, 14 and 21 after implantation, s.c., of an SW480 tumour. Injection of 2 $mg \cdot kg^{-1}$ of free DOX to mice (n = 6) bearing non-resistant tumours resulted in satisfactory antitumour activity and <10% relative weight loss within 35 days of tumour implantation (Figure 10A and B), suggesting the non-resistant tumour model was sensitive to DOX therapy. However, no significant changes in tumour growth and survival rate, as compared with the saline control, were obtained in mice, bearing SW480/DOX

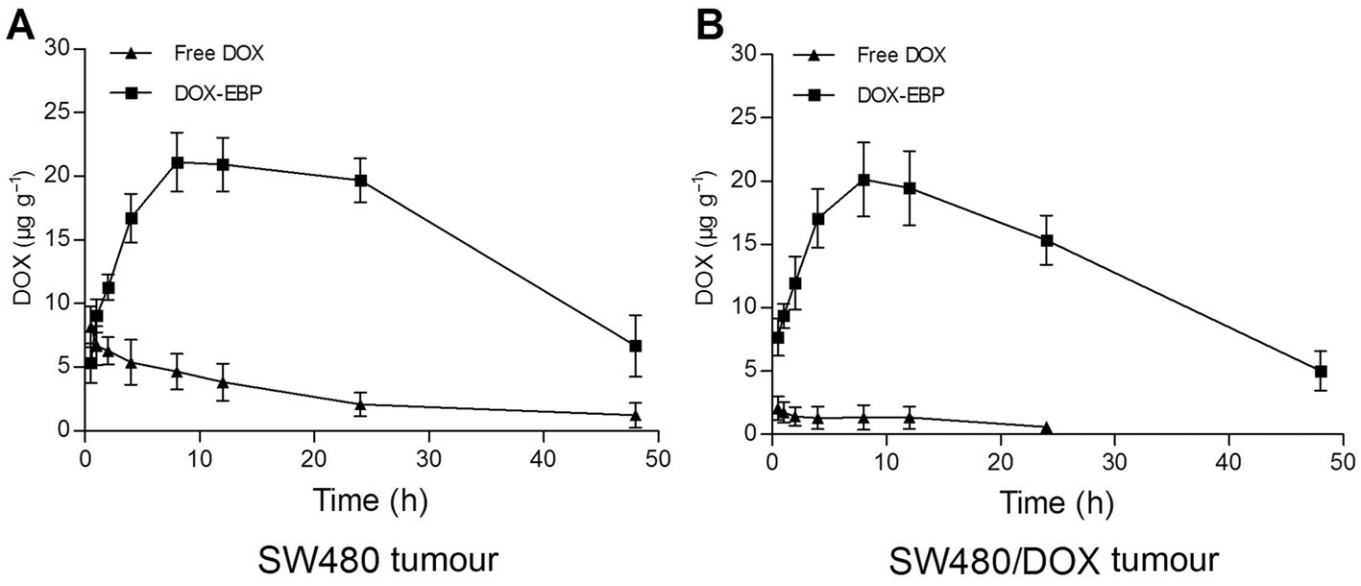

Figure 9

Tumour accumulation of free DOX and DOX-EBP conjugate in SW480 (A) and SW480/DOX (B) tumour-bearing BALB/c-nu/nu mice. Sections of tumours, 3 mm^3, were transplanted s.c. into experimental mice by a trocar needle. When tumours reached 550 mm^3, the animals were treated with a single dose of free DOX or DOX-EBP (5 $mg \cdot kg^{-1}$ DOX equivalent), and the DOX content of the tumour tissue was determined by HPLC of samples taken at the indicated times.

tumours, treated with free DOX in the same manner (Figure 10C and D). Thus, demonstrating the therapeutic failure of free DOX in DOX-resistant tumour model *in vivo*. In contrast, the tumour size in mice bearing non-resistant SW480 xenografts treated with DOX-EBP conjugate (15 $mg \cdot kg^{-1}$ of DOX equivalent) was decreased 9- and 16-fold as compared with that with free DOX (2 $mg \cdot kg^{-1}$) and saline, respectively, on day 35 (Figure 10A). In the DOX-resistant tumour model, the DOX-EBP conjugate was also more effective than free DOX, with the tumour size decreased 14- and 13-fold, respectively, as compared with the free DOX treatment and the saline control on day 35 (Figure 10C). In the survival assay performed in the non-resistant SW480 models (n = 6), all animals died in the saline group, two died in the free DOX group and none died in the DOX-EBP group on day 42 (Figure 10B). Similar survival results were also observed in the resistant SW480/DOX mouse models (Figure 10D). Taken together, these results demonstrate that the conjugation of DOX with EBP enhances the ability of DOX to inhibit solid tumour growth and increases the survival rate of both sensitive and resistant tumour models.

Discussion

DOX is one of the most commonly used anticancer drugs, but similar to most other anticancer chemotherapeutics, it has widespread systemic toxic effects on healthy tissues due to the lack of tumour selectivity. It is also well established that long-term use of DOX often leads to acquired resistance of cancer cells against a range of chemotherapeutic drugs, which in turn has limited its success in clinical chemotherapy. We have previously demonstrated that the DOX-EBP conjugate is able to target EGF receptor-overexpressing tumour cells (e.g. SW480 and SGC-7901) and to reduce non-specific side effects of DOX to normal tissues (Ai *et al.*, 2011). Using a DOX-resistant SW480/DOX cell line derived from its original SW480 cells, we now show that DOX-EBP can accumulate at high levels in DOX-resistant cells and prevent DOX resistance *in vitro* and *in vivo*.

A major cause of drug resistance in cancer chemotherapy is the increased expression and activity of P-gp in cancer cells, leading to reduced intracellular accumulation of drugs (Ozben, 2006). In this report, we show that the expression of P-gp expression significantly up-regulated (Figure 2), and the DOX accumulation is substantially decreased (Figure 1C) in the DOX-resistant SW480/DOX cells when treated with free DOX, as compared with that in non-resistant SW480 cells. These results are in agreement with the cytocidal effect of free DOX, which is potent against SW480 but not SW480/DOX cells (Figure 1A). Unlike free DOX, the DOX-EBP conjugate has almost the same cytocidal efficacy in both SW480 and SW480/DOX cells (Figure 3A). Consistently, the two types of cells retained similar levels of DOX-EBP (Figure 3C), which are comparable with that of free DOX in SW480 cells but much higher than that of free DOX in SW480/DOX cells (Figure 1C). These results indicate that the DOX-EBP conjugate, but not free DOX, can accumulate in cells regardless of their P-gp expression status and thus overcome the DOX resistance of SW480/DOX cells.

Based on the observation that most P-gp substrates are lipophilic and have a high propensity to partition into the lipid bilayer of cell membranes, P-gp has been proposed to recognize its substrates within the lipid bilayer (Aller *et al.*, 2009; Eckford and Sharom, 2009). As a hydrophobic small molecule, free DOX can easily diffuse into the lipid bilayer

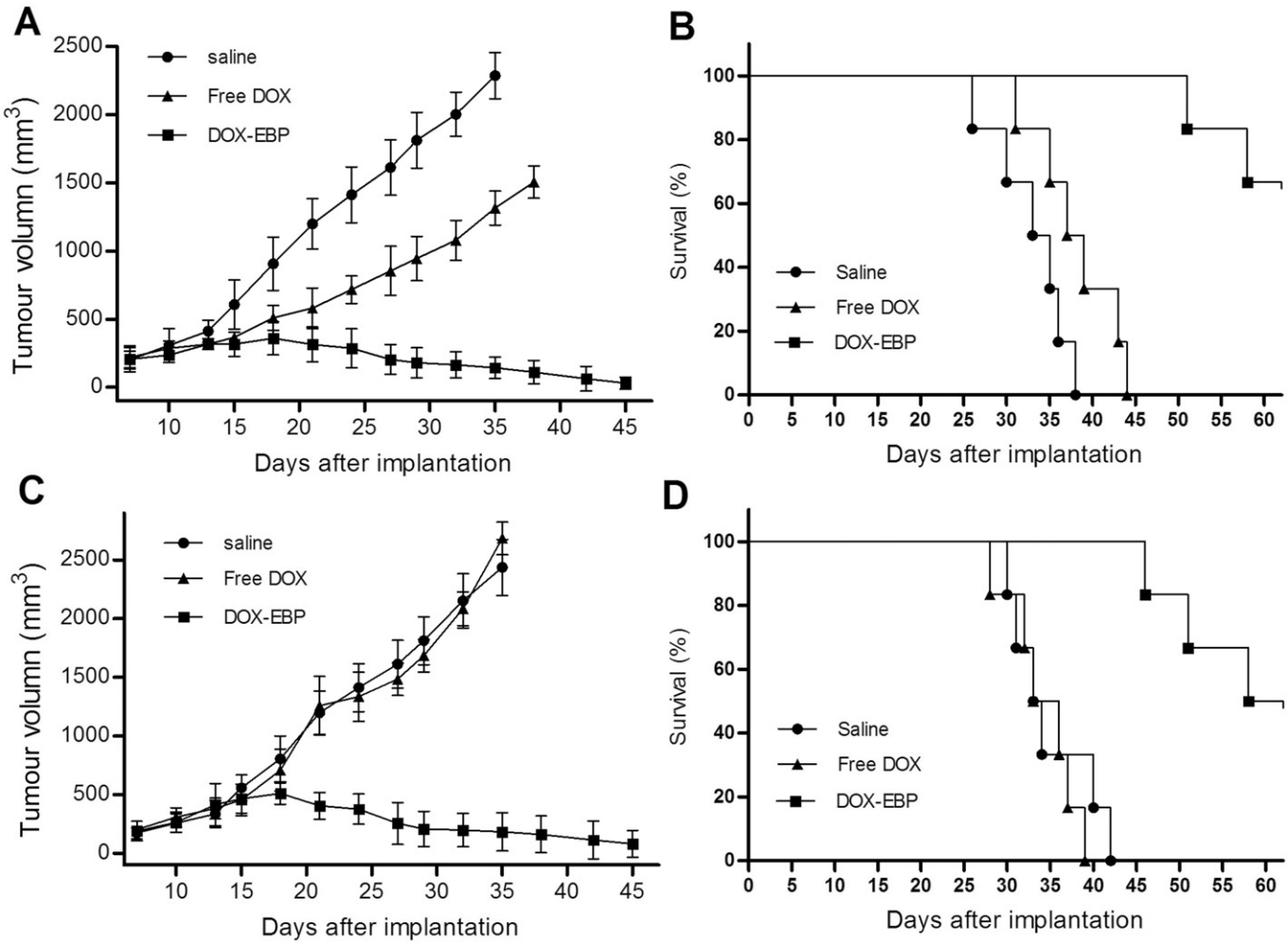

Figure 10

Therapeutic effect of free DOX and DOX-EBP conjugate in non-DOX-resistant SW480 and DOX-resistant SW480/DOX human colon cancer xenografts. Sections of tumours, 3 mm^3, were transplanted s.c. into BALB/c-nu/nu mice by a trocar needle and the mice were randomly divided into three groups (n = 6) treated with 2 $mg \cdot kg^{-1}$ of free DOX, 15 $mg \cdot kg^{-1}$ of DOX-EBP (DOX equivalent) or saline, injected into the tail vein on days 7, 14 and 21. (A and B) Effect of treating s.c. implanted SW480 xenograft with free DOX, DOX-EBP or saline showing tumour size (A) and Kaplan–Meier survival curves (B). (C and D) Effect of treating s.c. implanted SW480/DOX xenograft with free DOX, DOX-EBP or saline showing tumour size (C) and Kaplan–Meier survival curves (D).

but is also rapidly recognized and pumped out from DOX-resistant cells by the P-gp transporter (Figure 11A). However, the binding of DOX to carrier molecules may alter its pattern of cellular uptake. In particular, if DOX conjugates enter cells via receptor-mediated endocytosis, they are unlikely to be recognized and thus the P-gp efflux pump will be unable to remove them (Kim *et al.*, 2008). This is probably the case for the DOX-EBP conjugate (Figure 11B) since its cellular uptake can be inhibited by the anti-EGF receptor monoclonal antibody C225 and the endocytosis inhibitor PAO (Figure 6). Other findings from this study also support this notion. For example, a strong signal for DOX was present in both cytoplasm and nuclei of SW480 cells after 30 min and 24 h treatment with free DOX, indicating a passive diffusion of free DOX into the DOX-sensitive cells, but the DOX signal was much weaker in SW480/DOX cells under the same treatment, suggesting the efflux of free DOX in the DOX-resistant, P-gp-overexpressing cells (Figure 5). In contrast, treatment of both SW480 and SW480/DOX cells with DOX-EBP conjugate for 30 min led to the fluorescent DOX being distributed in the cytoplasm and perinuclear region, but after 24 h the fluorescence was observed in the nucleus (Figure 5), which is probably the result of DOX being released from the conjugate in the cytoplasm with the prolonged incubation and its subsequent entry into the nucleus. Together, these data indicate that the conjugation of DOX to EBP alters the cellular uptake process of DOX and that the EGF receptor-mediated endocytotic uptake of the conjugate helps DOX evade the effect of the P-gp efflux pump.

In addition to the *in vitro* cellular data, the *in vivo* experiments also showed that the drug level is higher in tumour tissue when the mice are administered the DOX-EBP conjugate than the free DOX. Following a single i.v. injection, the half-life of DOX-EBP in blood was longer than that of free

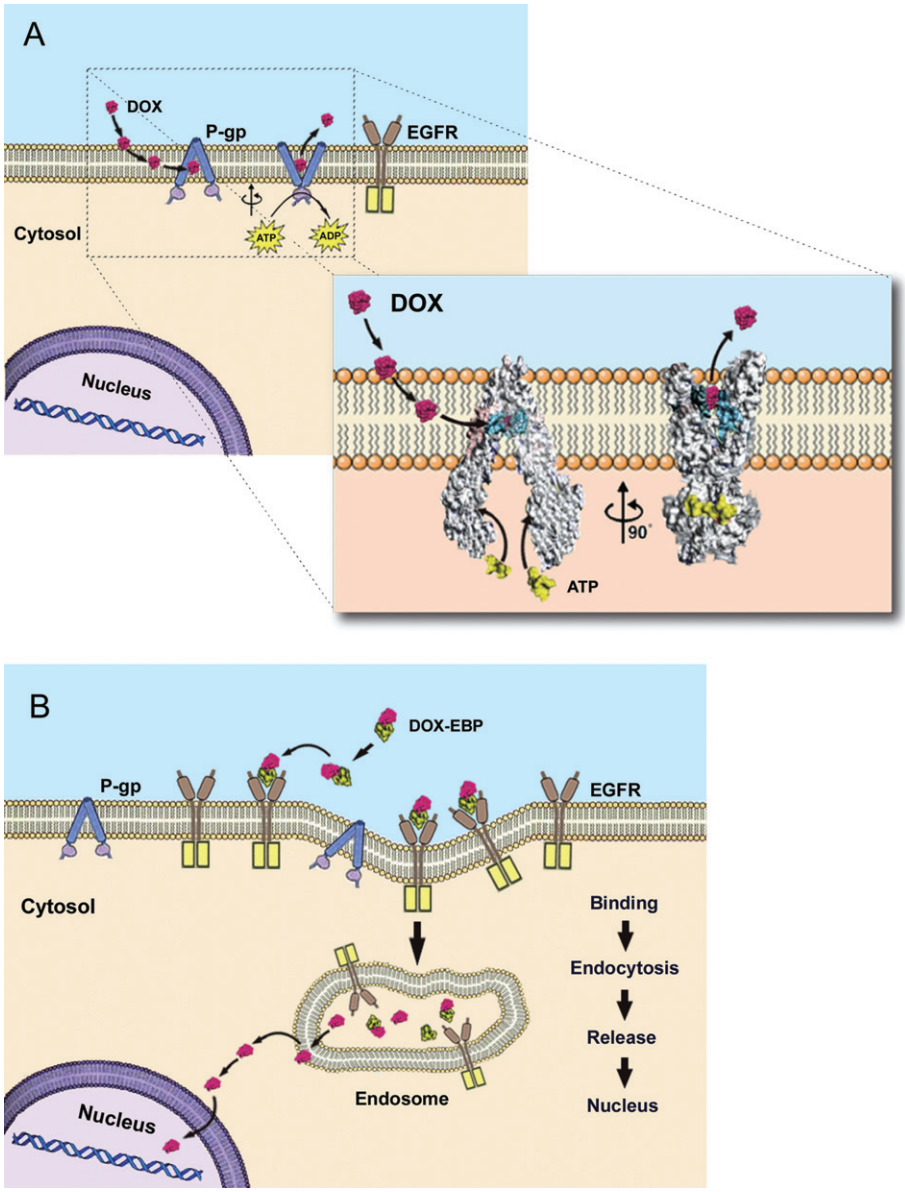

Figure 11

Internalization of DOX-EBP conjugate into P-gp-overexpressing cells via endocytosis. (A) Resistance model of cells to free DOX by P-gp pump (Aller *et al.*, 2009; Eckford and Sharom, 2009). The two cytoplasmic, nucleotide-binding domains (NBD) of P-gp polypeptide bind and hydrolyse ATP, while the two transmembrane domains (TMD) form a pathway for substrates to cross the plasma membrane. DOX approaching the cell is rapidly partitioned into the outer leaflet of the lipid bilayer and is closely bound to the drug-binding sites within the TMD. Then the cytosolic NBD is opened with the DOX-binding cavity formed by TMD facing towards the cytosol. This is followed by an ATP-dependent closure of the NBD and a concomitant alteration of P-gp to an outward-facing conformation, and the DOX is subsequently released outside of the cell. As a result, DOX is removed from the plasma membrane leaflet before entering the cell interior, leading to a lowered intracellular DOX level and thus drug resistance of the cell. (B) Cellular internalization model of DOX-EBP conjugate bypassing the P-gp pump. When approaching the extracellular side of the plasma membrane, the DOX-EBP conjugate cannot partition into the lipid bilayer and instead binds to the extracellular fragment of the EGF receptor (EGFR) on the cell surface, forming a receptor–conjugate complex. The conjugate is accumulated in an endosome and transported into the cell via receptor-mediated endocytosis. Once inside the cytoplasm, the conjugate is hydrolysed by a cellular esterase and the active DOX is released. Upon entering the nucleus, the DOX exerts its pharmacological action. Therefore, the DOX-EBP conjugate can bypass the P-gp pump by entering the DOX-resistant cell via receptor-mediated endocytosis and as a result overcomes the DOX resistance of the cell.

DOX, leading to an extended circulation time of the conjugate and consequently a higher AUC in the tumour tissue. In contrast, the DOX-EBP accumulation is lower than free DOX in normal tissues, including liver, lung, kidney and heart (Ai *et al.*, 2011). This type of targeted chemotherapy has been developed to selectively deliver cytotoxic agents to malignant cells and achieve a higher intratumoural concentration of drugs, leading to higher antitumour activity. Hence, we tested

the antitumour efficacy of DOX-EBP in a murine model bearing B16 melanoma and revealed the strong inhibitory effect of the conjugate on tumour growth (Ai *et al*., 2011). In the present study, we further showed that DOX-EBP has anti-tumour effects in mouse models bearing either non-DOX-resistant or DOX- resistant human colon cancer xenografts (Figure 10) and thus demonstrate that the conjugate successfully targets tumour cells *in vivo*.

In conclusion, this study has revealed that the conjugation of DOX to EBP alters the cellular uptake process of DOX and that the EGF receptor-mediated endocytotic uptake of the conjugate helps DOX evade the effect of the P-gp efflux pump. The DOX-EBP conjugate was also found to inhibit solid tumour growth and increase the survival rate of both sensitive and resistant tumour models. Together with our previous work, these findings demonstrate that the DOX-EBP conjugate has the potential to be a therapeutic agent for EGF receptor-overexpressing and DOX-resistant tumours and thus may provide a novel treatment for MDR cancer patients.

Acknowledgements

This work was supported by the National Natural Science Foundation of China (Grants 30971456, 30973664 and 21002074) and the National Basic Research Program of China (Grants 2010CB529804 and 2008CB418200).

Conflicts of interest

The authors declare no conflicts of interest.

References

Abbosh PH, Montgomery JS, Starkey JA, Novotny M, Zuhowski EG, Egorin MJ *et al*. (2006). Dominant-negative histone H3 lysine 27 mutant derepresses silenced tumor suppressor genes and reverses the drug-resistant phenotype in cancer cells. Cancer Res 66: 5582–5591.

Ai S, Duan J, Liu X, Bock S, Tian Y, Huang Z (2011). Biological evaluation of a novel doxorubicin-peptide conjugate for targeted delivery to EGF receptor-overexpressing tumor cells. Mol Pharm 8: 375–386.

Aller SG, Yu J, Ward A, Weng Y, Chittaboina S, Zhuo R *et al*. (2009). Structure of P-glycoprotein reveals a molecular basis for poly-specific drug binding. Science 323: 1718–1722.

Al-Shawi MK, Polar MK, Omote H, Figler RA (2003). Transition state analysis of the coupling of drug transport to ATP hydrolysis by P-glycoprotein. J Biol Chem 278: 52629–52640.

Aroui S, Brahim M, Kenani A (2010). Cytotoxicity, intracellular distribution and uptake of doxorubicin and doxorubicin coupled to cell-penetrating peptides in different cell lines: a comparative study. Biochem Biophys Res Commun 391: 419–425.

Bajo AM, Schally AV, Halmos G, Nagy A (2003). Targeted doxorubicin-containing luteinizing hormone-releasing hormone analogue AN-152 inhibits the growth of doxorubicin-resistant MX-1 human breast cancers. Clin Cancer Res 9: 3742–3748.

Bakos E, Evers R, Calenda G, Tusnády GE, Szakács G, Váradi A *et al*. (2000). Characterization of the amino-terminal regions in the human multidrug resistance protein (MRP1). J Cell Sci 24: 4451–4461.

Bidwell GL 3rd, Davis AN, Fokt I, Priebe W, Raucher D (2007). A thermally targeted elastin-like polypeptide-doxorubicin conjugate overcomes drug resistance. Invest New Drugs 25: 313–326.

Bild AH, Turkson J, Jove R (2002). Cytoplasmic transport of Stat3 by receptor-mediated endocytosis. EMBO J 21: 3255–3263.

Eckford PD, Sharom FJ (2009). ABC efflux pump-based resistance to chemotherapy drugs. Chem Rev 109: 2989–3011.

Gatlik-Landwojtowicz E, Aänismaa P, Seelig A (2006). Quantification and characterization of P-glycoprotein-substrate interactions. Biochemistry 45: 3020–3032.

Gottesman MM, Fojo T, Bates SE (2002). Multidrug resistance in cancer: role of ATP-dependent transporters. Nat Rev Cancer 2: 48–58.

Grandal MV, Madshus IH (2008). Epidermal growth factor receptor and cancer: control of oncogenic signalling by endocytosis. J Cell Mol Med 12: 1527–1534.

Higgins CF (2007). Multiple molecular mechanisms for multidrug resistance transporters. Nature 446: 749–757.

Kilkenny C, Browne W, Cuthill IC, Emerson M, Altman DG (2010). NC3Rs Reporting Guidelines Working Group. Br J Pharmacol 160: 1577–1579.

Kim D, Lee ES, Park K, Kwon IC, Bae YH (2008). Doxorubicin loaded pH-sensitive micelle: antitumoral efficacy against ovarian A2780/DOXR tumor. Pharm Res 25: 2074–2082.

Lee ES, Na K, Bae YH (2005). Doxorubicin loaded pH-sensitive polymeric micelles for reversal of resistant MCF-7 tumor. J Control Release 103: 405–418.

Liang JF, Yang VC (2005). Synthesis of doxorubicin-peptide conjugate with multidrug resistant tumor cell killing activity. Bioorg Med Chem Lett 15: 5071–5075.

Litman T, Zeuthen T, Svovgaard T, Stein WD (1997). Competitive, non-competitive and cooperative interactions between substrates of P-glycoprotein as measured by its ATPase activity. Biochim Biophys Acta 1361: 169–176.

Łubgan D, Józwiak Z, Grabenbauer GG, Distel LV (2009). Doxorubicin-transferrin conjugate selectively overcomes multidrug resistance in leukaemia cells. Cell Mol Biol Lett 14: 113–127.

Lurje G, Lenz HJ (2007). EGFR signaling and drug discovery. Oncology 77: 400–410.

McGrath J, Drummond G, Kilkenny C, Wainwright C (2010). Guidelines for reporting experiments involving animals: the ARRIVE guidelines. Br J Pharmacol 160: 1573–1576.

Meyer-Losic F, Quinonero J, Dubois V, Alluis B, Dechambre M, Michel M *et al*. (2006). Improved therapeutic efficacy of doxorubicin through conjugation with a novel peptide drug delivery technology (vectocell). J Med Chem 49: 6908–6916.

Ogawara K, Un K, Tanaka K, Higaki K, Kimura T (2009). In vivo anti-tumor effect of PEG liposomal doxorubicin (DOX) in DOX-resistant tumor-bearing mice: involvement of cytotoxic effect on vascular endothelial cells. J Control Release 133: 4–10.

Ozben T (2006). Mechanisms and strategies to overcome multiple drug resistance in cancer. FEBS Lett 580: 2903–2909.

Regev R, Yeheskely-Hayon D, Katzir H, Eytan GD (2005). Transport of anthracyclines and mitoxantrone across membranes by a flip-flop mechanism. Biochem Pharmacol 70: 161–169.

Riganti C, Miraglia E, Viarisio D, Costamagna C, Pescarmona G, Ghigo D *et al.* (2005). Nitric oxide reverts the resistance to doxorubicin inhuman colon cancer cells by inhibiting the drug efflux. Cancer Res 65: 516–525.

Rottenberg S, Nygren AO, Pajic M, van Leeuwen FW, van der Heijden I, van de Wetering K *et al.* (2007). Selective induction of chemotherapy resistance of mammary tumors in a conditional mouse model for hereditary breast cancer. Proc Natl Acad Sci U S A 104: 12117–12122.

Schinkel AH, Jonker JW (2003). Mammalian drug efflux transporters of the ATP binding cassette (ABC) family: an overview. Adv Drug Deliv Rev 55: 3–29.

Siarheyeva A, Lopez JJ, Glaubitz C (2006). Localization of multidrug transporter substrates within model membranes. Biochemistry 45: 6203–6211.

Wong HL, Bendayan R, Rauth AM, Xue HY, Babakhanian K, Wu XY (2006). A mechanistic study of enhanced doxorubicin uptake and retention in multidrug resistant breast cancer cells using a polymer-lipid hybrid nanoparticle system. J Pharmacol Exp Ther 317: 1372–1381.

Wu W, Luo Y, Sun C, Liu Y, Kuo P, Varga J *et al.* (2006). Targeting cell-impermeable prodrug activation to tumor microenvironment eradicates multiple drug-resistant neoplasms. Cancer Res 66: 970–980.

Yamochi T, Aytac U, Sato T, Sato K, Ohnuma K, McKee KS *et al.* (2005). Regulation of p38 phosphorylation and topoisomerase IIα expression in the B-cell lymphoma line Jiyoye by CD26/dipeptidyl peptidase IV is associated with enhanced in vitro and in vivo sensitivity to doxorubicin. Cancer Res 65: 1973–1983.

Zhang X, Chibli H, Mielke R, Nadeau J (2011). Ultrasmall gold-doxorubicin conjugates rapidly kill apoptosis-resistant cancer cells. Bioconjug Chem 22: 235–243.